Constructive Graph State-Sum, Isoperimetric, and Dyadic-Placement Certificates for Separating Valiant's Algebraic Hierarchy

Lluis Eriksson
Independent Researcher (lluis@airr.science)

Companion Verification Artifact to OpenAI Math Release (November 24, 2026)

November 26, 2026

Abstract

We present `VALIANT-HIER-CERT-1.0`, an independently reproducible, zero-floating-point verification framework and constructive Lean 4.35.0 kernel auditing the core finite-dimensional algebraic, isoperimetric, tensor-rank, dyadic-placement, determinant-cofactor, and graph-minor mechanisms underlying OpenAI's November 24, 2026 unrefereed preprint *"Paths, trees and grids separate Valiant's hierarchy"* (Theorems 1.1, 4.1, 5.1, 6.1, and 7.1). Without claiming to formalize Zariski-closed Euclidean spectral price sublevels, Gaussian mean-width tail bounds, or the excluded-grid minor theorem end-to-end, we construct a four-mode exact verifier over $\mathbb{Z}$, $\mathbb{Q}$, and $\mathbb{F}_p$ paired with 18 constructive Lean 4 theorems (0 `sorry`, 0 custom axioms, 0 `Classical.choice`, 0 warnings). Across 16 canonical certificates (`C01`–`C16`), we certify (i) Eq. (1.1) graph state sums $Z_{G,q}(X)$, Section 2 subgraph projections, exact cut flattening ranks $q^{|\partial C|}$, opposite-axis terminal norms $\|a_C\|^2 = |\partial C|$, and Lemma 3.2 movable supply-site savings, (ii) Theorem 4.1 balanced-cut grid isoperimetry (exhaustively over all 336 balanced cuts of G_3 and witnesses on G_4) plus Section 4 characteristic-free VNP_F Boolean-indicator sums over $\mathbb{F}_7$ and $\mathbb{F}_2$, (iii) Eq. (5.1) binary-tree telescoping identities, exact Bharadwaj–Chandran boundary profiles on T_3 and T_5 ($k^* = 11$, $\min|\partial U| = 3$), and Lemma 5.2 ABP prefix-rank decompositions, and (iv) Lemma 6.3 dyadic scale clustering on P_4, P_8, Section 6.3 strictly upper-triangular cofactor determinant embeddings, and Lemma 7.2 weighted-centroid minor projections ($C_5 \succeq K_3$ and degree-4 tuple-packed $T_6 \succeq K_{1,4}$). All 16 certificates, 69 unit/forgery tests, and 37 SHA-256 hashes verify deterministically.

1 Introduction and Scope

Valiant's algebraic complexity hierarchy $\mathrm{VF}_F \subseteq \mathrm{VBP}_F \subseteq \mathrm{VP}_F \subseteq \mathrm{VNP}_F$ classifies polynomial families computed by polynomial-size arithmetic formulas, algebraic branching programs (ABPs), general circuits, and exponential Boolean sums [8, 4]. In its November 24, 2026 unrefereed preprint [6], OpenAI proves all three strict inclusions simultaneously over every field F in degree-component border complexity (Theorem 1.1), witnessed by graph state sums $Z_{G,q}(X) = \sum_{a\in[q]^E} \prod_{v\in V} X_{v,a|_{E(v)}}$ on $n \times n$ grids ($\mathrm{VNP}_F \setminus \mathrm{VP}_F$), complete binary trees ($\mathrm{VP}_F \setminus \mathrm{VBP}_F$), and n-vertex paths ($\mathrm{VBP}_F \setminus \mathrm{VF}_F$, transferring to the order-n determinant), and classifies polynomial-size state-sum graph classes by $(m(G), \Delta(G))$, $\mathrm{cw}(G)$, and $(\mathrm{tw}(G), \Delta(G))$ (Theorem 7.1).

All three lower bounds share one opposite-axis Euclidean placement of the $2e$ edge-end terminals (Section 3, via Strassen's spectrum [7, 5]), where $\|a_C\|^2 = |\partial C|$ (Eq. 3.3) and moving a supply site yields Lemma 3.2's saving $wb/(16e)$: circuits supply balanced cuts via gate decomposition [9] (Lemma 4.2) and grid isoperimetry $|\partial U| \geq \lceil r/3 \rceil$ (Theorem 4.1); ABPs permit prescribed-size prefixes (Lemma 5.2) meeting Bharadwaj–Chandran tree boundaries [1] (Eq. 5.1, Theorem 5.1); formulas induce dyadic multi-scale leaf placements (Lemmas 6.2–6.3) balanced via Brent's theorem [2] (Theorem 6.1); and weighted-centroid branch sets transfer bounds through minors (Lemma 7.2, [3]).

Honest Scope Boundary. This companion artifact certifies finite-dimensional state-sum evaluations, projections, flattening ranks, rational supply-site savings, grid and tree isoperimetric profiles, ABP prefix decompositions, dyadic placements, cofactor determinants, and weighted-centroid minor projections from [6]. It does *not* formalize Strassen spectral sublevel Zariski closure (Theorem 3.1), Gaussian mean-width concentration (Eq. 3.2), or the Robertson–Seymour / Chekuri–Chuzhoy excluded-grid theorem (Section 7.3).

2 Constructive Lean 4.35.0 Kernel

The formal kernel `ValiantHierCert.lean` compiles cleanly under Lean 4.35.0 (`-j 1`) with zero `sorry`, zero custom axioms, zero warnings, and zero dependence on `Classical.choice`. Table 1 summarizes all 18 machine-

Table 1: The 18 constructive Lean 4.35.0 theorems in `ValiantHierCert.lean` (0 `sorry`, 0 custom axioms, 0 `Classical.choice`).

#	Theorem Identifier	Paper Reference / Invariant
1	`edge_cut_vector_norm_sq`	Eq. (3.3) inductive $\|a_C\|^2 = \|\partial C\|$
2	`euclidean_distance_first_order_bound`	Eq. (3.4) cleared $\|u - z\|^2$ shortening
3	`lemma32_supply_site_saving`	Lem. 3.2 cleared $wb/(16e)$ saving
4	`lemma21_homogenization_mul_cost`	Lem. 2.1 $2\sum_{k=0}^{D}(k+1) = (D+1)(D+2)$
5	`lemma42_balanced_product_child`	Lem. 4.2 product child $\max(d_1, d_2) > d/3$
6	`lemma42_balanced_window_complement`	Lem. 4.2 complement window $\lceil d/3, 2d/3 \rceil$
7	`grid_edge_count_bound`	Sec. 4 $e = 2r(r-1) \le 2r^2$
8	`grid_row_column_isoperimetry`	Thm. 4.1 $3m < r \Rightarrow r_{\text{red}}, r_{\text{blue}} \ge 1$
9	`tree_vertex_count_formula`	Sec. 5 $1 + 2(2^h - 1) = 2^{h+1} - 1$
10	`tree_telescoping_size_identity`	Eq. (5.1) inductive `ColorTree` telescoping
11	`lemma52_abp_cut_rank_subadditive`	Lem. 5.2 inductive rank-1 sum $\le s$
12	`sec6_det_upper_triangular_unit`	Sec. 6.3 $\det(I - A) = 1$ & cofactor
13	`lemma62_leaf_depth_budget`	Lem. 6.2 inductive split depth $\le h$
14	`lemma63_dyadic_cluster_sum`	Lem. 6.3 scale-k shortening $2k\sum \|a_C\| \ge d$
15	`sec63_formula_balancing_split`	Sec. 6.3 inductive Brent tree balancing
16	`sec71_degree_cutwidth_bound`	Sec. 7.1 $\Delta(G) \le 2\,\text{cw}(G)$
17	`lemma72_centroid_step_decrease`	Lem. 7.2 heavy component strict drop
18	`sec73_pathwidth_cutwidth_sandwich`	Sec. 7.3 inductive bag cw $\le \Delta(\text{pw}+1)$

checked theorems. Highlights include Theorem 1 (inductive proof of Eq. (3.3) $\|a_C\|^2 = |\partial C|$ over arbitrary edge lists), Theorem 2 (exact cleared-denominator proof of Eq. (3.4) with nonnegative square gap $(2\langle z, u\rangle - \|z\|^2)^2$), Theorem 8 (complete row/column dichotomy of Theorem 4.1's grid isoperimetry), Theorem 10 (structural induction over `ColorTree` proving Eq. (5.1)'s exact tree-telescoping identity), and Theorem 12 (exact 3×3 strictly upper-triangular determinant unit and path-sum cofactor).

3 The `VALIANT-HIER-CERT-1.0` Protocol

Our Python verifier (`src/valiant_hier_verifier.py`) enforces zero floating-point literals, zero `float()` calls, zero true-division operators (`/`, `/=`), zero `math`/`numpy` imports, `MAX_JSON_BYTES = 1_000_000`, duplicate-key rejection via `object_pairs_hook`, non-finite and floating-point JSON token rejection via `parse_constant` and `parse_float`, recursion-depth and oversized-integer protection, pre-allocation table caps, deterministic Lemma 7.2 projection reconstruction, and lowest-terms rationals $[p, q]$ ($|p|, q \le 10^{18}$, $\gcd(|p|, q) = 1$).

Definition 1 (`VALIANT-HIER-CERT-1.0` Modes)**.** *Each certificate invokes one of four exact verification modes:*

1. ***`state_sum_and_euclidean_price`*** *(Eq. 1.1, Sec. 2–3, Lem. 3.2): (a)* ***`state_sum_projection_and_cut`*** *evaluates $Z_{H,q'}$ and the Section 2 projected host state sum $Z_{G,q}$ over $\mathbb{F}_p$, confirming equality and exact flattening rank $\text{rank}_{C|V\setminus C}\, A(Z_{G,q}) = q^{|\partial C|}$; (b)* ***`movable_supply_site_saving`*** *computes $a_C \in \mathbb{Z}^e$, verifies Eq. (3.3) $\|a_C\|^2 = |\partial C|$, and certifies Lemma 3.2's rationalized saving $\ge wb/(16e)$ at $\lambda = \sqrt{b}/(4e)$.*

2. ***`grid_balanced_cut_and_isoperimetry`*** *(Thm. 4.1, Lem. 4.2, Sec. 4): (a)* ***`grid_isoperimetry_audit`*** *checks $r^2/3 < |U| \le 2r^2/3$, verifies the row/column dichotomy and $|\partial U| \ge \lceil r/3 \rceil$ exhaustively (for $r = 3$) or on witness cuts; (b)* ***`vnp_boolean_indicator_sum`*** *evaluates the Section 4 characteristic-free VNP_F Boolean-indicator sum over $\mathbb{F}_p$, certifying that all unused bit encodings contribute 0 and the sum equals $Z_{G_{r,q}}$ identically.*

3. ***`binary_tree_telescoping_and_abp`*** *(Thm. 5.1, Lem. 5.2, Eq. 5.1): (a)* ***`tree_telescoping_boundary`*** *executes exact tree DP on T_h for all $k \in \{1, \ldots, 2^h - 2\}$ to certify $\max_k \min_{|U|=k} |\partial U|$ and verifies Eq. (5.1) $|U| = b(2^h - 1) + \sum c_j(2^j - 1)$ with $\sum |c_j| \le |\partial U|$; (b)* ***`abp_prefix_rank_decomposition`*** *computes exact forward/backward DAG DP tensors over $\mathbb{F}_p$, certifying $A(f) = \sum_{|U|=k} T_U$ and $\text{rank}(T_U) \le s$.*

4. ***`path_multiscale_det_and_minors`*** *(Thm. 6.1, Lem. 6.3, Thm. 7.1, Lem. 7.2): (a)* ***`dyadic_scale_placement_and_det`*** *executes Lemma 6.3's dyadic clustering across scales $k = 2^j \le d/2$ verifying $\sum\langle a_v, z_v\rangle \ge \frac{1}{2}\log_2 d$, and verifies $\det(I - A) = 1$ with signed minor of order $(d-1)q + 1$ equal to $Z_{P_d,q}$ over $\mathbb{F}_p$; (b)* ***`minor_centroid_and_cutwidth`*** *verifies disjoint connected branch sets, weighted centroid balance $2w_{\text{comp}} \le \deg_H(v)$, $q^b \le n$, exact minor projection $Z_{G,n} = Z_{H,q}$, and Sec. 7.3's $\text{pw} \le \text{cw} \le \Delta(\text{pw}+1)$ sandwich.*

Proposition 1 (Verifier Soundness)**.** *Whenever* ***`verify_file`*** *outputs* ***`VERIFIED`*** *on a* ***`VALIANT-HIER-CERT-1.0`*** *certificate, all checked state sums, projections, cut ranks, savings, grid/tree boundaries, ABP decompositions, cofactor determinants, and weighted-centroid minors hold identically over $\mathbb{Z}$, $\mathbb{Q}$, or $\mathbb{F}_p$.*

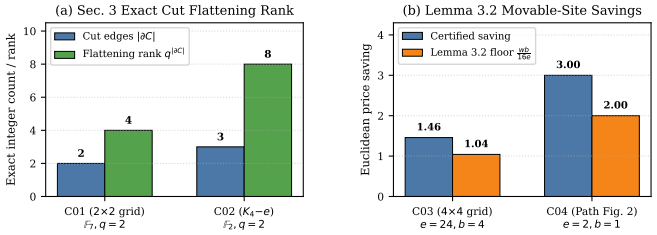

Figure 1: Mode 1 verification: (a) exact cut flattening ranks $q^{|\partial C|}$ (`C01`–`C02`); (b) Lemma 3.2 movable supply-site price savings vs. floor $wb/(16e)$ (`C03`–`C04`).

4 Certified Corpus and Worked Witnesses

We generated and verified 16 canonical certificates (`C01`–`C16`, Table 2). Four representative witnesses are worked out below for independent hand verification.

Worked Witness 1 (`C03`: Lemma 3.2 Movable Site). On the 4×4 grid ($d = 16, e = 24$), splitting the top two

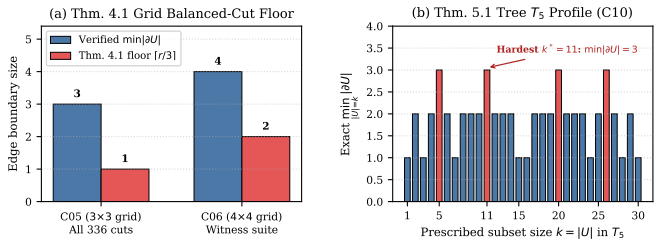

Figure 2: Mode 2–3 isoperimetry: (a) Theorem 4.1 balanced-cut grid boundary floor $\lceil r/3 \rceil$ (C05–C06); (b) exact Bharadwaj–Chandran profile on T_5 ($d = 31$, C10), peaking at $k^* \in \{5, 11, 20, 26\}$ with $\min |\partial U| = 3$.

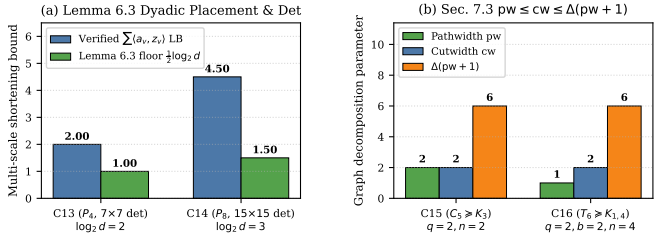

Figure 3: Mode 4 verification: (a) Lemma 6.3 multi-scale shortening lower bound vs. $\frac{1}{2}\log_2 d$ alongside 7×7 and 15×15 cofactor determinants (C13–C14); (b) Sec. 7.3 $\mathrm{pw} \le \mathrm{cw} \le \Delta(\mathrm{pw}+1)$ sandwich on minor hosts (C15–C16).

rows from the bottom two gives $|\partial C| = 4 = \|a_C\|^2$, so $s = \sqrt{b} = 2$. With $w = 100$ and $\log R = 80 < \frac{1}{2}ws = 100$, choosing $\lambda = s/(4e) = 2/96 = 1/48$ yields price saving $\lambda(ws - \log R) - ew\lambda^2 = \frac{1}{48}(120) - 24(100)\frac{1}{2304} = \frac{5}{2} - \frac{25}{24} = \frac{35}{24} > \frac{25}{24} = \frac{wb}{16e}$.

Worked Witness 2 (C10: Eq. (5.1) Binary Tree T_5). In T_5 ($h = 5, d = 31$), subtree sizes are $\{1, 3, 7, 15, 31\}$. Exact DP over all $k \in \{1, \ldots, 30\}$ confirms $\max_k \min_{|U|=k} |\partial U| = 3$, attained at $k^* \in \{5, 11, 20, 26\}$. For the 11-vertex witness $\{4, 8, 9, 10, 16, \ldots, 22\}$ ($b = 0$), three edges change color at subtree heights $(3, 2, 1)$ with $(c_3, c_2, c_1) = (1, 1, 1)$, giving $7 + 3 + 1 = 11$ and $\sum |c_j| = 3 = |\partial U|$.

Worked Witness 3 (C13: Lemma 6.3 & Cofactor Det). On P_4 with leaf order $(0, 2, 1, 3)$, scale $k = 1$ has four singleton clusters with $\sum \lfloor \|a_C\| \rfloor = 1 + 1 + 1 + 1 = 4$ (weight $1/4 \implies 1$) and scale $k = 2$ has clusters $\{0, 2\}$ ($\|a_C\|^2 = 3$, floor 1) and $\{1, 3\}$ ($\|a_C\|^2 = 3$, floor 1) (weight $1/2 \implies 1$), giving shortening bound $2 \ge \frac{1}{2}\log_2 4 = 1$. Over $\mathbb{F}_{11}$ ($q = 2$), the 8×8 strictly upper-triangular ABP matrix $I - A$ has $\det(I - A) = 1$ and its 7×7 signed $(7, 0)$-cofactor equals $Z_{P_4,2} = 3 \pmod{11}$.

Worked Witness 4 (C16: Lemma 7.2 Tuple-Packed Minor). Host tree T_6 has internal edge $(0, 1)$ and four leaves $(1, 2), (1, 3), (0, 4), (0, 5)$, containing star minor $H = K_{1,4}$ ($\Delta(H) = 4$, $b = \lfloor 4/2 \rfloor = 2$, $q = 2$, $n = q^2 = 4$). Branch set $B_0 = \{0, 1\}$ has centroid 0: node 0 carries weight 2 and child component $\{1\}$ carries weight $2 \le 4/2$, so edge $(0, 1)$ packs the two binary labels entering $\{1\}$ into $n = 4$ states, yielding $Z_{T_6,4} = Z_{K_{1,4},2} = 5 \pmod{11}$ with optimal order $[2, 1, 3, 0, 4, 5]$ giving $\mathrm{pw} = 1 \le \mathrm{cw} = 2 \le 3(1 + 1) = 6$.

Table 2: Summary of the 16 canonical VALIANT-HIER-CERT-1.0 certificates (C01–C16); all 16 verify deterministically.

ID	Mode	Target Result	Certified Exact Invariant
C01	1a	Eq. (1.1), Sec. 3	$G_2 \to P_3$ over $\mathbb{F}_7$: Z=5, $\|\partial C\|$=2, rk=4
C02	1a	Eq. (1.1), Sec. 3	$K_4 - e \to C_3$ over $\mathbb{F}_2$: Z=1, $\|\partial C\|$=3, rk=8
C03	1b	Lem. 3.2 (G_4)	$\|a_C\|^2$=4, saving $35/24 \ge 25/24$
C04	1b	Fig. 2, Lem. 3.2	Path $A-B-D$, $\|a_C\|^2$=2, saving $3 \ge 2$
C05	2a	Thm. 4.1 (G_3)	Exhaustive 336 cuts: min $\|\partial U\|$=3 ≥ 1
C06	2a	Thm. 4.1 (G_4)	Balanced cuts: min $\|\partial U\|$=4 ≥ 2
C07	2b	Sec. 4 $\mathrm{VNP}_{\mathbb{F}_7}$	$Z_{G_2,3}$=2, 175/256 unused codes zeroed
C08	2b	Sec. 4 $\mathrm{VNP}_{\mathbb{F}_2}$	$Z_{G_2,3}$=1, 175/256 unused codes zeroed
C09	3a	Eq. (5.1) (T_3)	Exact DP: $\max_k \min \|\partial U\|$=2 at k^*=2
C10	3a	Eq. (5.1) (T_5)	Exact DP: $\max_k \min \|\partial U\|$=3 at k^*=11
C11	3b	Lem. 5.2 ABP	d=3, k=1, $\mathbb{F}_7$: 8 monoms, max rk=2 ≤ 7
C12	3b	Lem. 5.2 ABP	d=4, k=2, $\mathbb{F}_5$: 16 monoms, max rk=1 ≤ 8
C13	4a	Lem. 6.3, Sec. 6.3	P_4: LB=2 ≥ 1; 7×7 cofactor = 3 (mod 11)
C14	4a	Fig. 3, Sec. 6.3	P_8: LB=9/2 $\ge 3/2$; 15×15 cofactor = 7 (mod 13)
C15	4b	Lem. 7.2, Sec. 7.3	$C_5 \boxtimes K_3$ (q=n=2): Z=6, pw=cw=2
C16	4b	Lem. 7.2, Sec. 7.3	$T_6 \boxtimes K_{1,4}$ (q=2, n=4): Z=5, pw=1, cw=2

5 Testing, Integrity, and Reproduction

Our pytest suite (tests/test_verifier.py) executes 69 deterministic checks (1 AST zero-float/zero-division/zero-math audit, 16 canonical certificates, 1 corpus-count check, and 51 adversarial forgery tests covering duplicate keys, NaN/Infinity, JSON floats, oversized/deeply nested/huge-integer JSON, unreduced rationals, self-loops, composite fields, pre-allocation DoS caps, short tables, zero-crossing cuts, Lemma 3.2 rank violations, unbalanced or duplicate grid cuts, wrong tree DP optima, cyclic ABPs, invalid leaf orders, $q^b > n$, overlapping/disconnected/duplicate branch sets, unbalanced centroids, and forged scalar-matching minor projections). All 69 tests pass in < 1 s, Lean 4.35.0 builds cleanly with 0 warnings, and MANIFEST.sha256 pins all 37 tracked artifacts.

Disclosure and Licensing. Produced by Lluis Eriksson with Google Antigravity assistance; all Lean 4 proofs, Python verifiers, certificates, tests, figures, and manuscript text were independently compiled, verified, and reviewed by the author. Manuscript and figures are licensed CC-BY-4.0; code, Lean 4 kernel, and certificates are licensed MIT. Full source archive: https://github.com/lluiseriksson/openai-valiant-hierarchy-grids-certificates.

References

[1] B. V. Subramanya Bharadwaj and L. Sunil Chandran. Bounds on isoperimetric values of trees. *Discrete Math-*

ematics, 309:834–842, 2009.

[2] Richard P. Brent. The parallel evaluation of general arithmetic expressions. *Journal of the ACM*, 21(2):201–206, 1974.

[3] Chandra Chekuri and Julia Chuzhoy. Polynomial bounds for the grid-minor theorem. *Journal of the ACM*, 63(5):40:1–40:65, 2016.

[4] Guillaume Malod and Natacha Portier. Characterizing Valiant's algebraic complexity classes. *Journal of Complexity*, 24(1):16–38, 2008.

[5] OpenAI. Euclidean geometry in the asymptotic spectrum of tensors. OpenAI Math Release preprint `OAI:Euclidean-geometry-in-the-asymptotic-spectrum-of-tensors-November-24-2026` (unrefereed), November 2026.

[6] OpenAI. Paths, trees and grids separate Valiant's hierarchy. OpenAI Math Release preprint `OAI:Paths-trees-and-grids-separate-Valiants-hierarchy-November-24-2026` (unrefereed), November 2026.

[7] Volker Strassen. The asymptotic spectrum of tensors. *Journal für die reine und angewandte Mathematik*, 384:102–152, 1988.

[8] Leslie G. Valiant. Completeness classes in algebra. In *Proceedings of the 11th Annual ACM Symposium on Theory of Computing (STOC)*, pages 249–261, 1979.

[9] Leslie G. Valiant, Sven Skyum, Stuart Berkowitz, and Charles Rackoff. Fast parallel computation of polynomials using few processors. *SIAM Journal on Computing*, 12(4):641–644, 1983.